Journal of Molecular Catalysis A: Chemical 341 (2011) 63–70

Contents lists available at ScienceDirect

Journal of Molecular Catalysis A: Chemical

journal homepage: www.elsevier.com/locate/molcata

On the regioselectivity of the insertion step in nickel complex catalyzed dimerization of butene: A density-functional study

Ioannis Nikiforidis, Andreas Görling, Wolfgang Hieringer*

Lehrstuhl für Theoretische Chemie, Department Chemie und Pharmazie, Universität Erlangen-Nürnberg, Egerlandstr. 3, 91058 Erlangen, Germany

ARTICLE INFO

Article history:
Received 23 September 2010
Received in revised form 17 March 2011
Accepted 26 March 2011
Available online 6 April 2011

Keywords:
Olefin dimerization
Selectivity
Density-functional theory
Homogeneous catalysis
Computational chemistry

ABSTRACT

The nickel complex catalyzed 1-butene dimerization to yield linear and branched C_8 olefins, a process of considerable industrial importance, is investigated with density-functional theory. Reaction energies and transition barriers have been calculated for the catalytic cycle of a nickel catalyst bearing two phosphine ligands. The data suggest olefin insertion as the rate determining step, and a hydrogen-transfer mechanism has been found as the most favorable chain termination step, in agreement with earlier studies on related systems. The olefin insertion step has subsequently been investigated in terms of its regioselectivity for three different ligands, i.e., the PH_3, PMe_3 and the N-heterocyclic carbene ligand IMe. The activation barriers for the IMe ligands are mostly found to be lower than those for phosphine ligands, indicating a higher catalytic activity of carbene complexes in butene dimerization. The computed relative transition state energies suggest that the PMe_3 and IMe ligands kinetically favor butene insertion into the primary Ni-butyl bonds, which leads to linear and singly branched C_8 products. Energetic differences in π-complexes may under non-equilibrium conditions lead to changes in selectivity towards branched product olefins when the catalyst bears IMe ligands.

1. Introduction

The production of higher olefins from simple bulk chemicals is a process of enormous technological importance. Several catalytic processes for the oligomerization of olefins have been developed and applied on the industrial scale, probably the most prominent examples being the homogeneous Shell higher olefins process (SHOP) developed by Keim and coworkers [1–3], or the homogeneous Dimersol process due to Chauvin and the heterogeneous Octol process [4].

These processes usually yield a mixture of several oligomeric products. A high selectivity for linear C_8 olefins (n-octenes, also methylheptenes) is of special interest in connection with the production of plasticizers or of linear low-density polyethylene (LLDPE) where they are used as co-monomers in ethylene polymerization [4]. Branched C_8 products are also of value as additives to increase the octane number of fuels [5]. This means even within the family of C_8 olefins control of the selectivity for the production of specific olefinic C_8 isomers is of considerable interest. One way to yield C_8 olefins is the dimerization of butene, which is the focus of the present work.

A number of active homogeneous catalyst systems for the oligomerization of α-olefins (including 1-butene) have been developed in the past. Nickel(II) complexes with O,O- or O,P-chelating ligands (such as F_6-acetylacetonate) are among the most successful catalysts for dimerization, but also phosphines and diimines have been employed as ligands in nickel catalysts [2]. The choice of the ligand affects the selectivity of the catalytic process, both in terms of the chain length of the products and the branching ratio (branched olefins vs. linear n-alkenes).

The mechanism of nickel-catalyzed olefin dimerization has been investigated in some detail [6]. The commonly accepted catalytic cycle (cf. Scheme 1) starts out from a nickel hydride complex as the active catalytic species which undergoes hydrometalation of the incoming (first) olefin molecule. The resulting nickel alkyl species then performs a (usually rate-determining) migratory insertion step with the incoming second olefin. This is the crucial carbon–carbon coupling step. In olefin dimerization (rather than oligomerization) the next major step involves a chain termination which yields the final di-olefin and which regenerates the catalytically active nickel complex.

The basic steps of olefin dimerization have also been investigated in theoretical studies. Fan and Ziegler have studied the dimerization of ethene via a nickel(II) acetylacetonato complex [7,8]. While the traditional steps of the catalytic cycle have been confirmed, an olefin-assisted β-hydrogen elimination step (also

* Corresponding author. Tel.: +49 9131 8528646; fax: +49 9131 8527736.
E-mail address: hieringer@chemie.uni-erlangen.de (W. Hieringer).

1381-1169/$ – see front matter © 2011 Elsevier B.V. All rights reserved.
doi:10.1016/j.molcata.2011.03.025

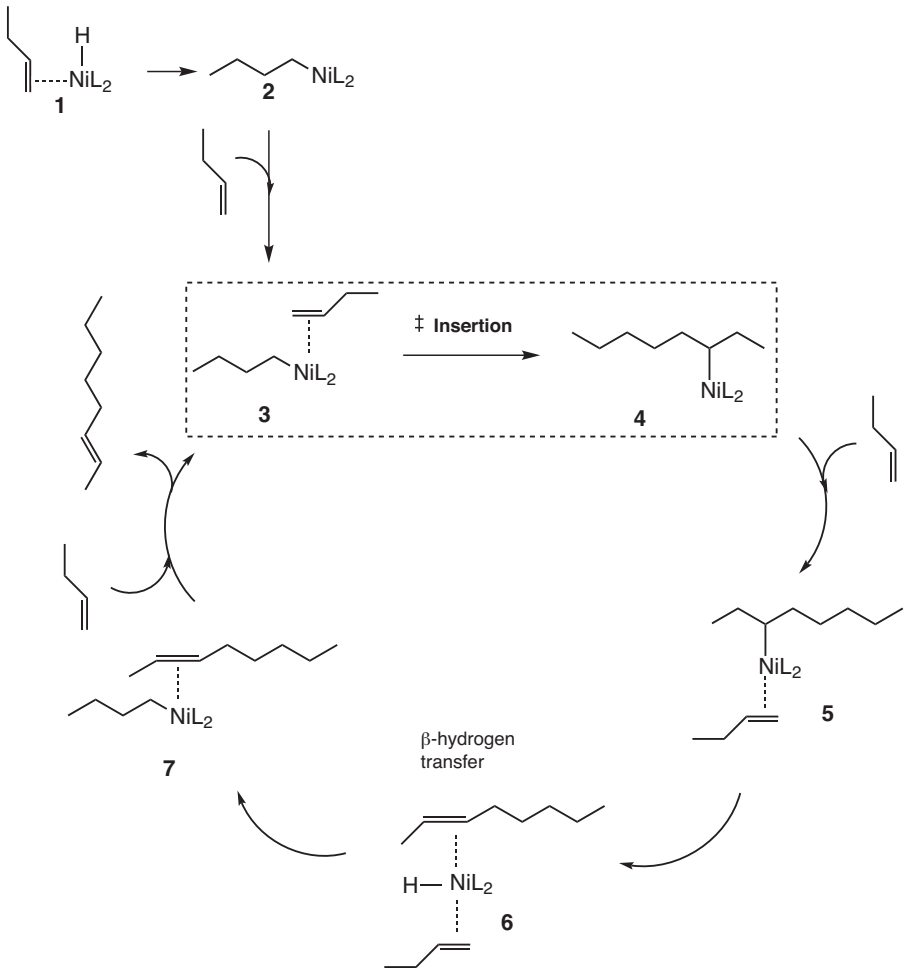

Scheme 1. Catalytic cycle considered for the catalytic dimerization of 1-butenes. L = monodentate ligand, e.g. phosphine or N-heterocyclic carbene (NHC). All structures with Ni carry a single positive charge.

called hydrogen transfer step) has been found to be more favorable than simple β-hydrogen elimination which had traditionally been assumed as the chain termination step. The carbon–carbon bond forming migratory insertion step has been confirmed as the rate-determining step of the catalytic cycle. The migratory alkene insertion step has received attention by theoreticians beyond olefin dimerization because this step is also crucial in olefin polymerization [9–11].

In this contribution, we focus on the regioselectivity of the dimerization of 1-butene catalyzed by cationic nickel(II) complexes which bear two classic spectator ligands, i.e., phosphines or N-heterocyclic carbenes (NHC). Beside their prominent role in various catalytic processes [12], such ligands have also been employed for olefin dimerization in so-called ionic liquids. For instance, the dimerization of propene has been studied using a nickel phosphine catalyst in an ionic liquid [5]. The cations in imidazolium-based ionic liquids have been reported as beneficial for the stability of the NHC-based catalyst [13]. The dimerization of butene by a $Ni(NHC)_2$ complex has also been investigated experimentally [14], yet various open questions concerning these ligand systems are yet not answered in sufficient detail. Herein, we put special emphasis on the regioselectivity of the migratory insertion step in the dimerization of 1-butene catalyzed by cationic nickel(II) complexes as a function of the ligands, i.e., two phosphine or NHC ligands. Since the catalyst system considered in this work has not been studied theoretically before, we start with an investigation of the basic steps of the catalytic cycle. We then proceed to the migratory insertion step, which is assumed to control the selectivity of the process. Our goal is to better understand the effects of ligands on the branching level of the resulting C_8 products obtained from nickel-catalyzed butene dimerization.

2. Computational details

The calculations are based on density-functional theory [15] (DFT) using both the gradient-corrected exchange-correlation functionals due to Becke [16] and Perdew [17] (denoted BP) in combination with the resolution-of-the-identity (RI) technique as well as the B3LYP [18] hybrid functional. A standard polarized triple-zeta split-valence basis set (TZVP) [19] from the Turbomole basis set library has been used in combination with the appropriate auxiliary basis set for the RI [20]. We have found that the BP and B3LYP functional yield analogous reaction energies and transition barriers in most cases. We quote the BP numbers here and refer to the Supplementary Material for the B3LYP numbers. Cases where BP and B3LYP are in disagreement are pointed out in the text. It should be noted that the energy differences which control the selectivities in this study are rather small (of the order of 1 kcal/mol), which represents a considerable challenge for present-day density functionals. In general, all intermediates and transition states have been fully optimized without any symmetry or other constraints. Strict convergence criteria for the geometry optimizations have been applied such as to ensure that the reaction energies and activation barriers are converged to below 0.1 kcal/mol (see

Table 1
Calculated (free) reaction energies ($\Delta E/\Delta G$) and activation barriers ($\Delta E^{\neq}/\Delta G^{\neq}$) of important steps of the catalytic cycle as shown in Scheme 1 (L = PH_3); kcal/mol.

Step	$\Delta E/\Delta G$	$\Delta E^{\neq}/\Delta G^{\neq}$
Butene insertion **3** → **4**	−11.2/−12.4	16.4/16.4
Butene coordination **4** → **5**	−5.7/+6.9[a]	–/–
Hydrogen transfer **5** → **6**	+7.4/+7.8	8.4/8.2[b]
Hydrogen transfer **6** → **7**	−6.4/−5.8	3.4/3.4[b]
Olefin exchange **7** → **3**	−3.1/−4.2	–/–

[a] Bimolecular reaction yielding a single product molecule, hence the free energy reflects the loss of rotational and translational entropy in the hypothetic gas-phase reaction. Energy obtained when omitting the translational and rotational entropies: −8.3 kcal/mol.
[b] See Ref. [24].

the Supplementary Material for details). The stationary points have been characterized as energy minima or transition states by means of frequency calculations. In general, several stereoisomers can be distinguished along reaction paths yielding the same C_8 dimerization products. For each path towards a particular C_8 isomer we have optimized several diastereomeric transition states and selected that transition state which is associated with the lowest activation barrier for the chosen C_8 isomer. All energies quoted include the corresponding zero-point vibrational energy. Free energies have been calculated from the standard gas-phase (ideal gas) formulae for room temperature (298.15 K) and ambient pressure (0.1 MPa); the calculated vibrational frequencies have not been scaled. No solvent effects have been included in the present calculations. All calculations have been performed with the Turbomole program package [21,22]. In this work, all nickel complexes are to be understood as cationic (charge +1).

3. Results

3.1. The catalytic cycle: reaction energies and kinetic barriers

Scheme 1 shows the catalytic cycle which the present work is based on. The active species in catalytic butene dimerization as considered here are cationic Ni(II) complexes with two "spectator" ligands L. We employ the simplest phosphine L = PH_3 for a survey of the catalytic cycle in order to identify the rate-determining step. To study the selectivity of the process we subsequently include also PMe_3 and the NHC ligand IMe for a more elaborate study on the olefin insertion step.

The catalytic cycle shown in Scheme 1 is consistent with earlier works on ethylene and propene dimerization [7,8,10,23]. It comprises hydrometalation steps (**1** → **2**, **6** → **7**), olefin insertion into Ni–C bonds (**3** → **4**), di-olefin (C_8 product) elimination by assisted β-H-elimination (β-H-transfer **5** → **6** → **7**) as well as olefin coordination or exchange reactions (**2** → **3**, **4** → **5**, **7** → **3**).

The reaction energies calculated for butene dimerization with L = PH_3 are collected in Table 1. The central step in olefin dimerization is the olefin insertion step into the Ni–alkyl bond (**3** → **4**) which is exothermic by 11.2 kcal/mol ($\Delta E = -11.2$ kcal/mol; $\Delta G = -12.4$ kcal/mol). It is associated with a substantial activation barrier of $\Delta E^{\neq} = 16.4$ kcal/mol ($\Delta G^{\neq} = 16.4$ kcal/mol). For olefin dimerization, it is important that this step occurs only once because a repeated insertion of olefins would lead to undesired oligomerization products. The olefin dimer therefore must be released via a chain termination process which is faster than repeated insertion. Our present results for butene dimerization confirm earlier findings by Fan and Ziegler [7,8] for ethylene oligomerization that an olefin-assisted β-H-transfer process (**5** → **6** → **7**) is energetically more favorable than an unassisted β-H-elimination from **4**. The activation barriers for β-H-transfer are calculated to $\Delta E^{\neq}_{\mathbf{5}\to\mathbf{6}} = 8.4$ kcal/mol ($\Delta G^{\neq}_{\mathbf{5}\to\mathbf{6}} = 8.2$ kcal/mol) and $\Delta E^{\neq}_{\mathbf{6}\to\mathbf{7}} = 3.4$ kcal/mol ($\Delta G^{\neq}_{\mathbf{6}\to\mathbf{7}} = 3.4$ kcal/mol), while that of unassisted β-H-elimination from **4** is calculated to $\Delta E^{\neq} = 15.0$ kcal/mol ($\Delta G^{\neq} = 16.0$ kcal/mol) [24]. β-H-transfer **5** → **7** is furthermore calculated as almost thermoneutral ($\Delta E = +1.0$ kcal/mol, $\Delta G = +2.0$ kcal/mol), while unassisted β-H-elimination from **4** leads to a π-complex intermediate (not shown in Scheme 1) of relatively high energy ($\Delta E = +7.9$ kcal/mol, $\Delta G = +8.7$ kcal/mol).

The relatively low barriers computed for chain termination via β-H-transfer, which are lower than the insertion barrier, thus suggest that the overall process is selective for olefin dimerization rather than oligomerization (subject to the assumption that repeated insertion reactions show similar barriers as those give for the first insertion as given above). The remaining steps in the catalytic cycle constitute olefin coordination and exchange processes such as **7** → **3**. We have not calculated activation barriers for these steps because olefin exchange may be assumed to occur via associative mechanisms and correspondingly low activation barriers [25–28]. Hence, we here assume them as being fast and do not consider them any further in this work [29].

Our present results in summary are consistent with the view that olefin insertion is the rate-determining step of the catalytic cycle for butene dimerization by cationic Ni(II) phosphine complexes for L = PH_3. This is in agreement with expectations from earlier experimental work and also matches results from previous theoretical studies on ethylene dimerization [7,8].

3.2. Butene insertion

We now focus on the migratory insertion step **3** → **4** (Scheme 1, cf. Fig. 1 for molecular structures) of 1-butene into the Ni–butyl bond which in the following is assumed to determine the selectivity of the overall catalytic cycle, i.e., the distribution of olefinic C_8 products yielded by the catalytic dimerization. As shown in Scheme 2, four basic variants are considered which may occur depending on the history of the catalyst in previous catalytic turnovers.

The first two lines in Scheme 2 represent (2,1)- and (1,2)-insertions into the primary Ni–butyl bond (Ni–C_{prim}) which occurs if the hydrometalation step **1** → **2** or **6** → **7** (see Scheme 1) in the previous catalytic turnover has proceeded with anti-Markovnikov regiochemistry. The last two lines show insertion into the Ni–C bond of a secondary butyl group. Such Ni–C_{sec} bonds are formed when the preceding hydrometalation steps have proceeded with Markovnikov regiochemistry. The C_8 products obtained from the four regiochemically different insertion variants given in Scheme 2 are either linear n-octenes or branched heptenes, hexenes, and pentenes (from **4a**: 2-octene or 3-octene; from **4b**: 2-ethyl-1-hexene; from **4c**: 5-methy-2-heptene or 5-methyl-3-heptene; from **4d**: 2-ethyl-3-methyl-1-pentene) [30]. In the following we study the effect of the monodentate ligands L = PH_3, PMe_3 (trimethylphosphane), and IMe (N,N′-dimethylimidazol-2-yliden) on the relative energetics of these insertion reactions. Figs. 2–4 provide graphical representations of the overall insertion free energy profiles for the four different insertion pathways shown in Scheme 2 for each of the three ligands.

3.2.1. Thermodynamics

Figs. 2–4 show that butene insertion is an exothermic and exoergic process for all variants shown in Scheme 2 and for all ligands. (The calculated reaction energies and free enthalpies of reaction of all insertion variants are collected in Table S1 in the Supplementary Material.) A comparison of the numbers given in Figs. 2–4 (see also Table S1) furthermore shows that insertion is more exothermic with the NHC ligand (L = IMe) than with the phosphines (exothermicity IMe > PMe_3 > PH_3). For all L, (2,1)-insertion

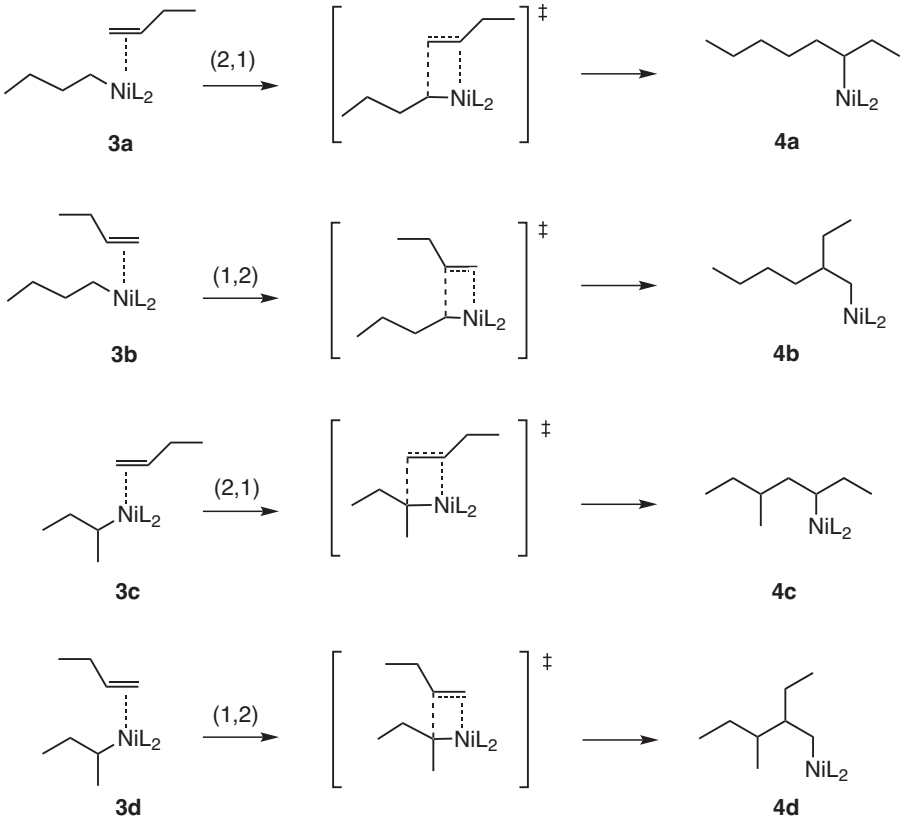

Scheme 2. (1,2)- and (2,1)-regiochemistry of the insertion of 1-butene to primary and secondary Ni–butyl bonds. Left: olefin complex reactands; center: transition states; right: insertion products; L = PH_3, PMe_3, IMe; all structures carry a single positive charge (not shown).

turns out to be slightly more exothermic than (1,2)-insertion. For L = IMe, the (2,1)-insertion into the Ni–C_{sec} bond (**3c** → **4c**) of the secondary butyl group somewhat breaks rank because it is considerably more exothermic (exoergic) than all concurring reactions (cf. Table S1 of the Supplementary Material).

3.2.2. Activation barriers and kinetic selectivity

The regioselectivity of butene insertion within the catalytic cycle is determined by the relative magnitudes of the (free) activation barriers of the insertion variants shown in Scheme 2. For each transition state formula given in the center column of Scheme 2 four diastereomeric transition state configurations can be distinguished which in general lead to different activation barriers although they represent paths to the same $L_2Ni(C_8)$ insertion product. The most competitive path leading to a particular C_8 product species is of course the one which is associated with the lowest activation barrier. For our analysis of the regioselectivity we have therefore calculated all possible transition states and selected those associated with the lowest energy found for each of the reactions given in Scheme 2. The corresponding (free) activation barriers for reactions **3** → **4** are collected in Table 2 (cf. also Figs. 2–4). The selected transition structure and intermediates for insertion **3a** → **4a** are

Table 2
Activation barriers $\Delta E^{\neq}$ /free energies of activation $\Delta G^{\neq}$ for the various insertion steps **3** → **4** (**a**–**d**) from Scheme 2; kcal/mol.

L	Ins **a** (2,1)	Ins **b** (1,2)	Ins **c** (2,1)	Ins **d** (1,2)
PH_3	16.4/16.4	16.9/16.6	17.1/16.4	18.3/18.8
PMe_3	15.3/15.5	14.8/15.0	15.6/15.0	17.0/16.9
IMe	13.6/13.7	13.9/14.4	12.2/13.1	12.5/10.9

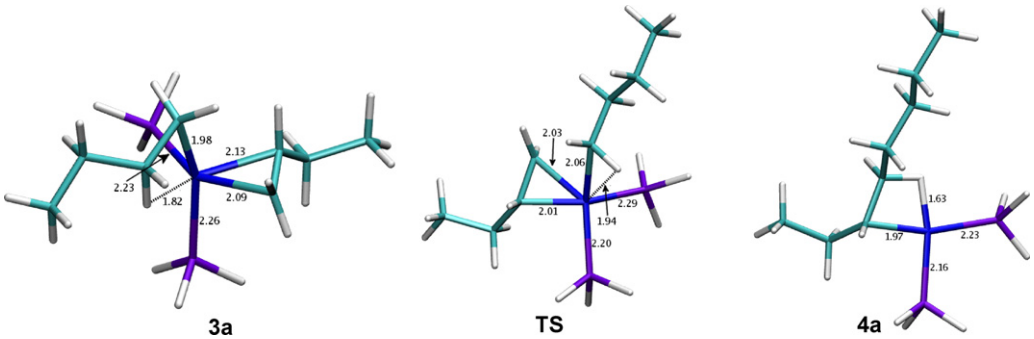

Fig. 1. Optimized geometries of complexes **3a** (left) and **4a** (right) as well as the associated insertion transition state (center) for L = PH_3, illustrating β-agostic interactions in **3a** and **4a** and an α-agostic interaction in the transition state (TS); color code: Ni = dark blue, P = violet, C = light blue, H = white; numbers represent bond distances (in Å) of ligator atoms (H, C, P) to Ni. See the Supplementary Material for further illustrations. (For interpretation of the references to color in this figure legend, the reader is referred to the web version of this article.)

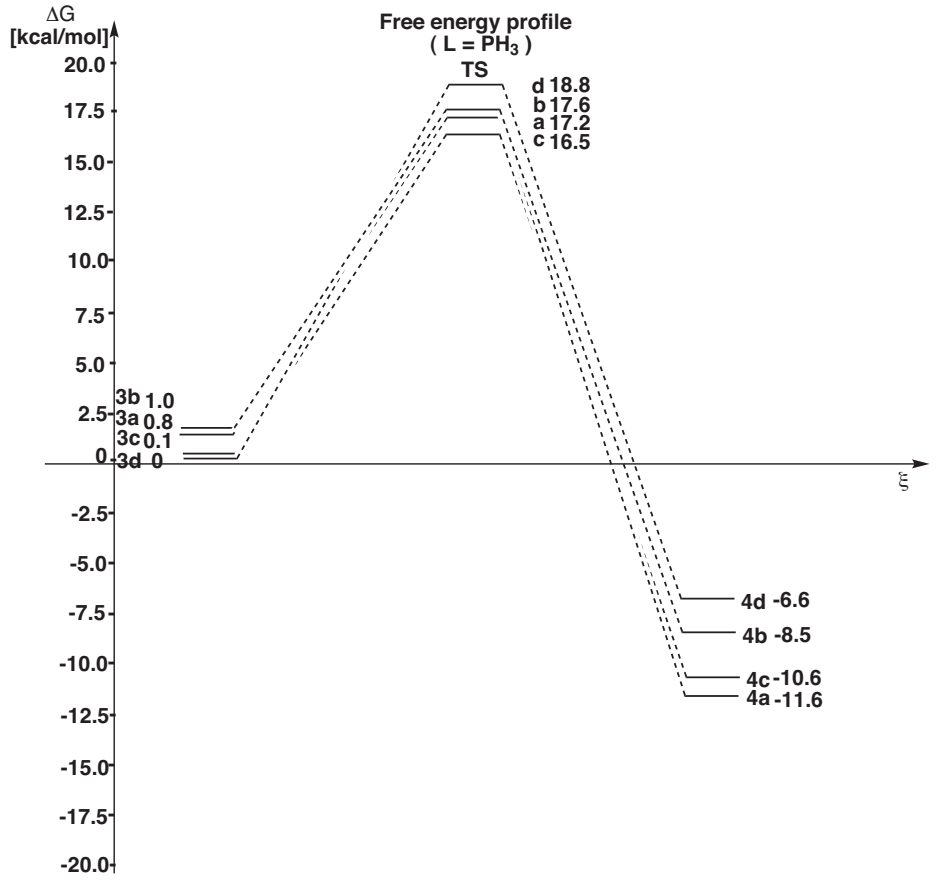

Fig. 2. Free energy diagram of the four different pathways given in Scheme 2 for L = PH_3.

depicted in Fig. 1 as an example (structures for the other pathways are provided in the Supplementary Material).

As a general trend, the activation barriers decrease in the series PH_3 > PMe_3 > NHC. In particular, all barriers for L = IMe are found to be lower than for the phosphine ligands, i.e., the catalyst is expected to be more active with NHC ligands. Furthermore, the calculations with the BP functional predict that butene insertion to the secondary butyl groups of **3c**, **3d** is kinetically favored over insertion to the primary butyl complexes **3a**, **3b** for L = IMe. (The latter observation is not confirmed at the B3LYP level, however, see the Supplementary Material for details.) The lowest barrier is found for **3c** → **4c** (L = IMe). For L = PMe_3, PH_3, on the other hand, less pronounced differences in activation barriers are found. For L = PH_3, insertion of butene to the primary butyl complexes **3a** and **3b** is predicted to be kinetically slightly favored over insertion from the secondary butyl complexes **3c**, **3d** (BP functional).

It is furthermore interesting to compare the difference in free energies of the π-complexes **3a**–**3d** relative to that π-complex with the lowest free energy. It can be seen from Figs. 2 and 3 that the free energies of the π-complexes are similar within 1.0 kcal/mol for L = PH_3 and within 2.1 kcal/mol for L = PMe_3. Larger differences up to 5.6 kcal/mol are calculated for L = IMe (Fig. 4), i.e., for this ligand π complexes **3a**, **b** with primary butyl groups are lower in energy than **3c**, **d** which bear a secondary butyl group. This in part explains the slightly lower activation barriers found for butene insertion to **3c**, **d** (Table 2, Fig. 4) because the π-bond of the olefin with the nickel center does not play a role in the transition state (cf. Section 3.2.3 below; cf. also the Supplementary Material for deviating B3LYP numbers). Under conditions of thermodynamic equilibrium, we therefore expect the majority of the catalyst molecules in resting states **3a** or **3b** for L = IMe, PMe_3.

To further analyze the ligand effect on butene insertion, we directly compare the transition state free energies for each of the insertion pathways (Scheme 2) without reference to the π-complexes **3**. These data can be taken from Figs. 2–4 (center part), for each L. The transition state free energies fall within 2.3 kcal/mol for L = PH_3, within 3.4 kcal/mol for L = PMe_3, and within 2.5 kcal/mol for L = IMe (similar trends, but larger spreads are found using the B3LYP functional, see the Supplementary Material for details). The transition states for insertion to secondary butyl groups (paths **c**, **d** in Scheme 2) are slightly higher in energy than those for insertion to primary butyl groups for the larger ligands L = PMe_3, IMe.

3.2.3. *Structural aspects of intermediates and transitions states*

Before analyzing the consequences of the calculated energetic data on the predicted regioselectivity, we discuss some interesting structural aspects of the intermediates and transition states involved in the insertion reactions. Fig. 1 shows the optimized geometries for the π-complex **3a**, the insertion product **4a** and the associated transition state for L = PH_3 as a representative example (for more illustrations see the Supplementary Material). The π-complexes **3** in general show a distorted tetrahedral geometry around the nickel center for L = PH_3, PMe_3. For L = IMe (again, see the Supplementary Material), an approximately square-planar coordination geometry is found where the double bond of the butene ligand and the planes of the NHC ligands are approximately perpendicular to the coordination plane. The insertion products **4** show a square-planar coordination, where the fourth (vacant) coordination site is occupied by a β-agostic interaction.

Agostic interactions are known to play a prominent role for the energetics of complexes of the present type (strength estimated to 12–14 kcal/mol for Ni) as has been pointed out before

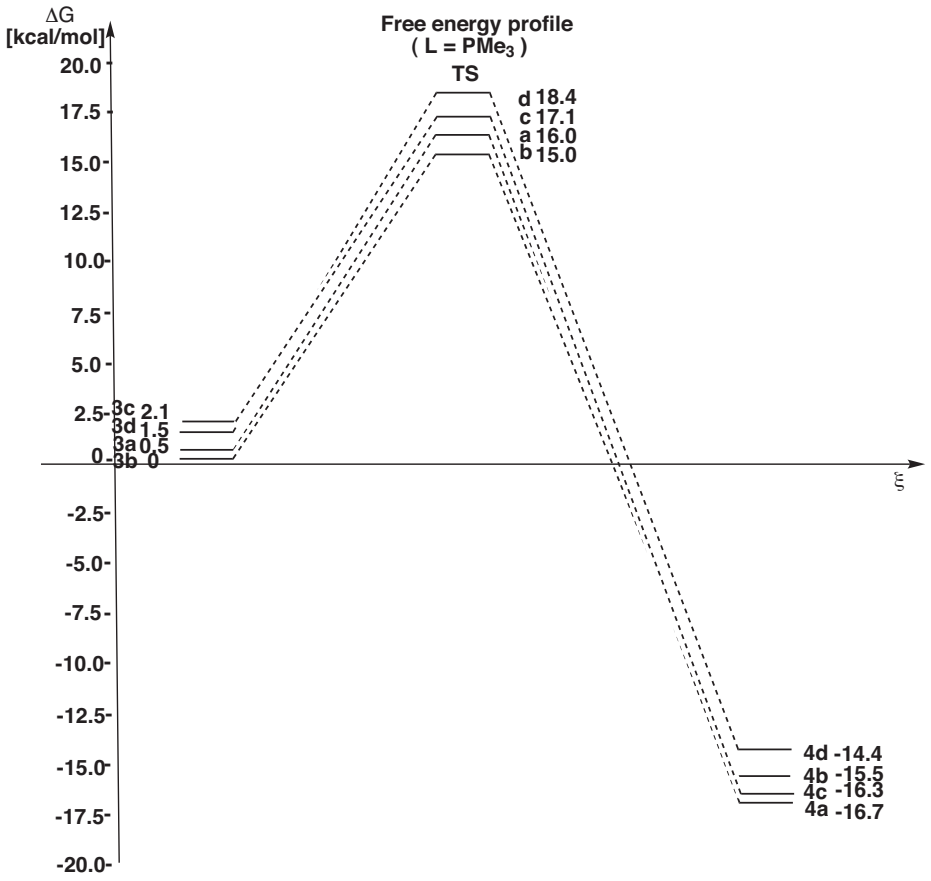

Fig. 3. Free energy diagram of the four different pathways given in Scheme 2 for L = PMe_3.

[9,23,31]. Their prevalence depends on the nature of the ligand, however. For L = PH_3, PMe_3 all complexes **3** and **4** are stabilized by β-agostic interactions due to the butyl group. A comparison with non-agostic isomers gives an estimated stabilization energy of roughly 5 kcal/mol due to the agostic interactions. β-Agostic interactions are also found for complexes **4** in the case of L = IMe. On the other hand, for L = IMe the corresponding complexes **3** do not show any agostic interactions in their lowest-energy geometries. Furthermore, in the transition states connecting **3** and **4**, for none of the three ligands pronounced β-agostic interactions are found. Instead, these are replaced by α-agostic bonds in most cases (see the Supplementary Material for illustrations).

The presence or absence of agostic interactions and the differences among the ligands L can be rationalized by considering the electronic situation at the Ni center. The NHC ligands are generally considered strong donors which therefore lower the propensity of Ni to accommodate an additional agostic bond. The insertion products **4** are coordinatively unsaturated, however, and the vacant fourth coordination site is consequently occupied by an agostic bond for all L.

4. Discussion

We now discuss the regioselectivity of the insertion process which results from the calculated energetics presented in the previous section. In order to qualitatively predict selectivity trends based on the above data, we distinguish two limiting cases. In the first (standard) case, we assume that all steps shown in Scheme 1 are fast compared to the insertion reaction(s) and hence the isomeric π-complex species **3a**–**d** are in thermodynamic equilibrium with each other. This assumption is compatible with the calculated energetics of the steps in the catalytic cycle for standard concentrations. The interconversion among **3a**–**d** can proceed via ligand exchange processes such as the equilibrium **3** ↔ **7** (Scheme 1) and via β-hydrogen transfer steps similar to the interconversion between **6** and **7** shown in Scheme 1. From basic kinetic arguments [32] it then follows that the relative barrier heights associated with the concurring insertion reactions shown in Scheme 2 are given by the relative transition state energies for insertions **a**–**d** which are shown in the center of Figs. 2–4 (see also the Table S5 in the Supplementary Material). We have shown above that for L = PMe_3, IMe the absolute transition state energies tend to be lower for butene insertion into the Ni–C_{prim} bond of a primary butyl group (insertions **a** and **b**) as compared to insertion into the secondary butyl bond (both BP and B3LYP levels; the only, notable exception is L = PH_3, which favors **3c** → **4c** at the BP level). This preference is especially pronounced for the NHC ligand. Considering the overall dimerization reaction, this results in a preference for linear octene and singly-branched 2-ethyl-1-hexene products rather than doubly-branched products. For L = PMe_3, moreover a slight preference for (1,2) insertion from **3b** to yield 2-ethyl-1-hexene is predicted by the present calculations (cf. Fig. 3).

As a second case it is also interesting to consider the special situation where **3a**–**d** are not in thermodynamic equilibrium with each other, such that reactions from each species **3** can be considered as an independent reaction channel. (Admittedly, such a hypothetical situation might rarely occur as long as isomerization via β-H-transfer is fast.) In such cases the rates of butene insertion for each species **3a**–**d** are determined by the activation energies given in Table 2, i.e., by the differences in (free) energy of the π-complexes and corresponding transition states. From Table 2, the activation barriers are higher for insertion path **d** (2,1-insertion to a secondary

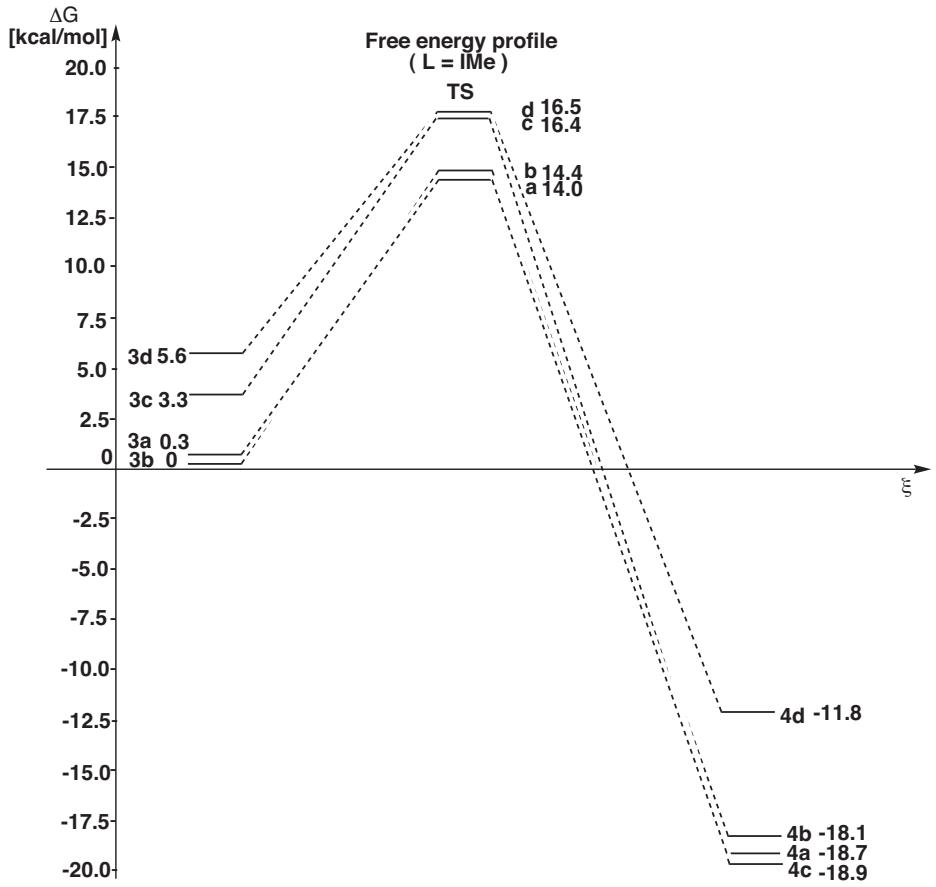

Fig. 4. Free energy diagram of the four different pathways given in Scheme 2 for L = IMe.

butyl group, cf. Scheme 2) for L = PH_3, PMe_3. (Less clear trends are found at the B3LYP level, however. See the Supplementary Material for details.) The similar magnitude in activation barriers is paralleled by similar energies of the π-complexes for L = PH_3 or PMe_3 (cf. Figs. 2 and 3). In essence this makes us arrive at similar selectivity predictions as discussed above for L = PH_3 and PMe_3, i.e., a tendency towards linear or singly branched C_8 products. For L = IMe, however, the situation is different. The activation barriers given in Table 2 clearly favor insertion into the Ni–C_{sec} bond of the secondary butyl complexes **3c**, **d** (BP functional; B3LYP again less pronounced). This is due to the fact that for L = IMe the π complexes **3** have rather different energies, see Fig. 4, and hence the order of activation barriers varies considerably from the order of transition state energies. Hence, for L = IMe based on the present calculations we expect a change in selectivity in favor of the singly or doubly branched dimerization products 5-methyl-2-heptene (or 5-methyl-3-heptene) and, in particular, 2-ethyl-3-methyl-1-pentene in the hypothetical case of equal (i.e., non-equilibrium) concentrations of π-complexes **3a**–**d** in the catalytic system.

5. Conclusions

We have studied the dimerization of 1-butene catalyzed by cationic nickel(II) phosphine and N-heterocyclic carbene complexes $[RR'NiL_2]^+$ (R = butyl, R′ = 1-butene) by means of density functional calculations, with a special focus on the regioselectivity of the insertion step of the catalytic cycle. As a first step, we have calculated the (free) reaction energies and barriers of all crucial steps in the basic catalytic cycle for the dimerization of butene. The butene insertion step is associated with a higher activation barrier than chain termination and other steps and is therefore assumed to represent the rate-determining step of the catalytic cycle in this work, in agreement with earlier studies on ethylene and propene dimerization. Moreover, the β-hydrogen transfer step was confirmed as a likely chain-termination mechanism also for butene dimerization.

The main focus in this study was to investigate the ligand dependence of the regioselectivity of the rate-determining insertion step and thus the selectivity for linear and branched C_8 products in 1-butene dimerization. To this end, we have calculated the thermodynamic reaction energies and kinetic activation barriers for four regiochemically different insertion steps, which represent (1,2) and (2,1) insertion to primary and secondary Ni–C bonds. Three different ligands have been considered, i.e., two phosphines (PH_3, PMe_3) and the N-heterocyclic carbene IMe. According to the catalytic cycle assumed, the butene insertion step can take place from four isomeric π-complex reactands which are in equilibrium with each other for standard conditions due to fast isomerization processes. In general, the barriers for insertion with IMe ligands are found to be lower than for phosphine ligands, indicating a higher activity of IMe complexes in butene dimerization. For L = PMe_3 and L = IMe we furthermore find slightly lower activation barriers for insertion into primary Ni–C bonds, indicating a kinetic preference in favor of linear or singly branched C_8 products. For L = IMe, we furthermore find that the π-complex resting states from which butene insertion takes place have different energies depending on whether a primary or a secondary butyl group is bound to the nickel center. This is associated with lower insertion barriers for those π complexes which bear a secondary butyl group. In the hypothetical case where isomerization among the various π-complex reactands is slow this fact may lead to a bias towards highly branched C_8

products for L = IMe. In general, the insights from this study can be of use to improve the selectivity of nickel-catalyzed butene dimerization and hence to control the branching level of C_8 products via the choice of ligand additives.

Acknowledgements

The authors gratefully acknowledge the support of the Cluster of Excellence 'Engineering of Advanced Materials' at the University of Erlangen-Nuremberg, which is funded by the German Research Foundation (DFG) within the framework of its 'Excellence Initiative'. We thank Berthold Melcher and Peter Wasserscheid for bringing this topic to our attention, and Thorsten Wölfle for excellent computer services.

Appendix A. Supplementary data

Supplementary data associated with this article can be found, in the online version, at doi:10.1016/j.molcata.2011.03.025.

References

[1] M. Peuckert, W. Keim, Organometallics 2 (1983) 594–597.
[2] W. Keim, Ed. Angew. Chem. Int. 29 (1990) 235–244.
[3] B. Cornils, W.A. Herrmann, Applied Homogeneous Catalysis with Organometalic Compounds, Wiley-VCH, Weinheim, 2000.
[4] A. Brückner, U. Bentrup, H. Zanthoff, D. Maschmeyer, J. Catal. 266 (2009) 120–128.
[5] Y. Chauvin, S. Einloft, H. Olivier, Ind. Eng. Chem. Res. 34 (1995) 1149–1155.
[6] W. Keim, New J. Chem. 11 (1987) 531.
[7] L. Fan, A. Krzywicki, A. Somogyvari, T. Ziegler, Inorg. Chem. 33 (1994) 5287–5294.
[8] L. Fan, A. Krzywicki, A. Somogyvari, T. Ziegler, Inorg. Chem. 35 (1996) 4003–4006.
[9] S. Strömberg, K. Zetterberg, P.E.M. Siegbahn, J. Chem. Soc. Dalton Trans. (1997) 4147–4152.
[10] A. Michalak, T. Ziegler, Organometallics 19 (2000) 1850–1858.
[11] H. von Schenck, S. Strömberg, K. Zetterberg, M. Ludwig, B. Akermark, M. Svensson, Organometallics 20 (2001) 2813–2819.
[12] S. Diez-Gonzalez, N. Marion, S.P. Nolan, Chem. Rev. 109 (2009) 3612–3676.
[13] D.S. McGuinness, W. Mueller, P. Wasserscheid, K.J. Cavell, B.W. Skelton, A.H. White, U. Englert, Organometallics 21 (2002) 175–181.
[14] B. Ellis, W. Keim, P. Wasserscheid, Chem. Commun. (1999) 337–338.
[15] W. Koch, M.C. Holthausen, A Chemist's Guide to Density Functional Theory, 2nd ed., Wiley-VCH, Weinheim, 2000.
[16] A.D. Becke, Phys. Rev. A 38 (1988) 3098.
[17] J.P. Perdew, Phys. Rev. B 33 (1986) 8822.
[18] A.D. Becke, J. Chem. Phys. 98 (1993) 5648.
[19] F. Weigend, R. Ahlrichs, Phys. Chem. Chem. Phys. 7 (2005) 3297–3305.
[20] K. Eichkorn, O. Treutler, H. Öhm, M. Häser, R. Ahlrichs, Chem. Phys. Lett. 240 (1995) 283–290.
[21] R. Ahlrichs et al., TURBOMOLE 5.9, University of Karlsruhe, Karlsruhe, since 1988; www.turbomole.com.
[22] R. Ahlrichs, M. Bär, M. Häser, H. Horn, C. Kölmel, Chem. Phys. Lett. 162 (1989) 165.
[23] L. Deng, P. Margl, T. Ziegler, J. Am. Chem. Soc. 119 (1997) 1094–1100.
[24] The transition states for the β-H-transfer **5** → **6** → **7** could only be located using slightly more sloppy convergence criteria for the transition state search than the strict criteria which have been used for the remaining calculations. (Energy change below 10^{-5} a.u. rather than 10^{-6} a.u.).
[25] J.D. Atwood, Inorganic and Organometallic Reaction Mechanisms, 2nd ed., VCH, New York, 1997.
[26] L. Cattalini, in: M.L. Tobe (Ed.), Reaction Mechanisms in Inorganic Chemistry, Butterworths, London, 1972, pp. 269–302.
[27] A. Dedieu, Chem. Rev. 100 (2000) 543–600.
[28] C.H. Langford, H.B. Gray, Ligand Substitution Processes, Benjamin, New York, 1965.
[29] Note that (unassisted) olefin dissociation energies can be substantial, but such steps are not integral parts of the catalytic cycle assumed here.
[30] The position of the double bond in the C_8 products is of minor importance in the light of industrial applications where isomerization steps are usually performed subsequently. We therefore consider only one double bond regioisomer here.
[31] M.D. Leatherman, S.A. Svejda, L.K. Johnson, M. Brookhart, J. Am. Chem. Soc. 125 (2003) 3068–3081.
[32] K.J. Laidler, Chemical Kinetics, McGraw Hill, New York, 1991.